



Comparison of measured values on ^{11}C -methionine and ^{18}F -fluorodeoxyglucose PET obtained with two different scanners in normal brain and brain tumor

異なる2台のPET装置より得た正常脳実質および脳腫瘍での ^{11}C -メチオニンおよび ^{18}F -FDG PETの測定値の比較検討

Yu-ichi Yamada^{1), 2)}, Yoshitaka Asano^{2), 3)}, Seisuke Fukuyama¹⁾,
Ryo Tanokura^{1), 2)}, Yuka Ikegame^{2), 3)}, and Jun Shinoda^{2), 3)}

1) Chubu Medical Center for Prolonged Traumatic Brain Dysfunction, Kizawa Memorial Hospital, Department of Radiotechnology
2) Department of Clinical Brain Sciences, Gifu University Graduate School of Medicine
3) Chubu Medical Center for Prolonged Traumatic Brain Dysfunction, Kizawa Memorial Hospital, Department of Neurosurgery

Key words: PET, acquisition system, SUV, T/N ratio, brain tumor

【Abstract】

OBJECTIVE. The purpose of this study is to investigate if there were differences between the measured values obtained with 2-dimensional (2D-system) versus 3-dimensional acquisition system (3D-system) in positron emission tomography (PET) scans of the normal brain and brain tumors. **MATERIALS AND METHODS.** PET scanning with ^{11}C -methionine (MET-PET) or ^{18}F -fluorodeoxyglucose (FDG-PET) was performed using two scanners which were equipped with 2D-system and 3D-system. In 121 patients with various types of brain tumors, Regions of interest were placed in the normal brain structures and the standard uptake values (SUVs) were measured. In 35 patients with diffuse astrocytoma and 18 patients with meningioma, the tumor/normal brain ratio (T/N ratio) was calculated using the maximum SUV of the tumors and the mean SUV of the normal frontal cortex. **RESULTS.** The mean SUV of the normal brain structure acquired on the 3D-system was significantly lower than those on 2D-system for both MET and FDG-PET. The mean T/N ratio of diffuse astrocytoma from 3D-system was significantly lower than that from 2D-system with MET-PET, but there was no significant difference in the T/N ratio with FDG-PET in both brain tumors. **CONCLUSION.** This study suggest that with tumors in which the SUV was higher than that of the normal brain, which resulted in a lower T/N ratio obtained with 3D-system than that with 2D-system. With tumors in which the SUV was equal to or lower than that of the normal brain, which resulted in a T/N ratio obtained with 3D-system was approximately equal to that with 2D-system.

【要旨】

【背景および目的】本研究の目的は、2D収集機構および3D収集機構のPET装置（以下、2D-PET、3D-PET）から得られた正常脳および脳腫瘍の測定値の差を比較検討することである。【方法】 ^{11}C -メチオニンおよび ^{18}F -FDGを用い、2Dおよび3D-PETで121例の脳腫瘍患者を撮像し、正常脳に関心領域を設定してSUVを測定した。35例のびまん性星細胞腫、18例の髄膜腫の患者で腫瘍のSUVmaxと正常脳のSUVmeanを測定し、腫瘍-正常脳比（T/N比）を算出した。【結果】3D-PETの正常脳のSUVmeanは、 ^{11}C -メチオニンおよび ^{18}F -FDGのいずれにおいても2D-PETより有意に低かったが、FDG-PETより得たT/N比はいずれの脳腫瘍でも両装置間の差は有意でなかった。【結論】腫瘍のSUVが正常脳のSUVより高い場合に2Dおよび3D-PETのT/N比に差が生じる可能性が示唆された。

PURPOSE

Diagnosis of brain tumor by molecular imaging is essential for the evaluation of malignancy, prognosis, and to suggest a strategy for treatment¹⁻¹¹⁾. Also, for brain tumors, a number of studies that report the use PET scanning have been published. In this decade, our group has published several studies of brain tumors and related diseases in which PET was

used as the critical diagnostic modality¹²⁻¹⁵⁾. Recently, the number of clinics that use PET scanners has increased. At the present time, there are five medical equipment production companies producing PET scanners in the world. We need more comparative discussions regarding PET imaging of brain tumors obtained from different types of scanners worldwide in the literature and at meetings. In such settings, the data obtained from the different PET scanners used in the various institutes may not correspond. This issue should be noted and the measured values should be investigated. In our hospital, we had been using an ADVANCE NXi (NXi) Imaging System, equipped with a 2D acquisition system, and then transitioned to an Eminence STARGATE (SG), which

山田 裕一^{1), 2)}, 浅野 好孝^{2), 3)}, 福山 誠介¹⁾,
田野倉 亮^{1), 2)}, 池亀 由香^{2), 3)}, 篠田 淳^{2), 3)}

- 1) 自動車事故対策機構中部療護センター 木沢記念病院放射線技術部
- 2) 岐阜大学大学院医科学専攻脳病態解析学分野
- 3) 自動車事故対策機構中部療護センター 木沢記念病院脳神経外科

Received December 5, 2017; accepted April 27, 2018

is equipped with a 3D acquisition system. There was a large amount of accumulated data in brain tumors, which could be compared and differences in the data characteristics obtained from the two different PET scanners could be evaluated. To the best of our knowledge, there are no previous investigations comparing brain tumor imaging from a 2D acquisition system to that from a 3D acquisition system. The purpose of this study is to investigate if there were differences between the measured values obtained with 2D versus 3D acquisition systems from PET scanners in the normal brain and brain tumors.

MATERIALS AND METHODS

PET scanner

Data used in this study were obtained from two different PET scanners. One was an ADVANCE NXi Imaging System equipped with a 2D acquisition system that provided 35 transaxial images at 4.25 mm intervals with an in-place spatial resolution (full width on transaxial images) of 4.8 mm and an aperture width of the Z-axis direction of 150 mm (General Electric Yokogawa Medical Systems, Hino, Tokyo, Japan) (NXi), which had been used from 2006 to 2011. The other scanner was an Eminence STARGATE equipped with a 3D acquisition system that provided 99 transaxial images at 2.65 mm intervals with an in-place spatial resolution (full width on transaxial images) of 3.5 mm and an effective visual field of the Z-axis direction of 260 mm (Shimadzu Corporation, Kyoto, Japan) (SG), which has been used since 2011. The PET radiotracers, ^{11}C -methionine (MET) and ^{18}F -fluorodeoxyglucose (FDG) were used in this study. **Table 1** indicates the mechanical characteristics of these two scanners.

Patients

4,602 patients with brain tumors received PET scans in the Chubu Medical Center for Prolonged Traumatic Brain Dysfunction, Kiza-

Table 1 Summary of the characteristics of the two PET scanners

	NXi	SG
Equipped detector	BGO	GSO
Detector size (mm)	4.25×35	3.25×99
Aperture width (mm)	150	260
Acquisition system	2D	3D
Special resolution (mm)	4.2	3.5
Reconstruction	OS-EM	DRAMA
Iteration	2	1
Subset/Filter Cycle	14	128
Matrix	128×128	128×128

wa Memorial Hospital from July 2006 to March 2013. Among them, 121 randomly selected patients with various types of localized small brain tumors were enrolled in this study for the evaluation of the measured values on PET in normal brain structures. For the PET scanning, the NXi was used in 66 patients (mean age: 42.3 ± 13.6 years, 33 males) and the SG was used in 55 patients (mean age: 44.2 ± 14.5 years, 33 males). In addition, another 35 patients with diffuse astrocytoma (DA) and 19 patients with meningioma (MEN) that had the tumor type histologically confirmed were also enrolled in this study. For the PET scanning in patients with DA, the NXi was used in 20 patients (mean age: 47.4 ± 16.3 years, 10 males) and the SG in 15 patients (mean age: 44.5 ± 19.9 years, 8 males). For PET scanning in patients with MEN, the NXi was used in 13 patients (mean age: 68.0 ± 10.6 years, 4 males) and the SG in 6 patients (mean age: 63.5 ± 24.2 years, 1 male). Patients with DA or MEN were included in this study because these tumor types were representative tumors in which the radiotracer uptake within the lesions is homogeneous from our experience. No patients had undergone prior surgeries or adjuvant therapies. The study was approved by the institutional review board (27-025), and all subjects signed a written informed consent [or need for written informed consent was waived].

Data acquisition on PET

Participants were placed in the PET scanner so that axial slices were parallel to the cantho-

mental line, and the head was fixed to reduce body movement during the scan. In the NXi, a germanium-68 gallium rotating pin source was used to obtain a 3-min transmission scan and the radiopharmaceutical (MET: 5.0 MBq/kg, FDG: 5.0 MBq/kg) was injected intravenously via the cubital vein. With the MET-PET, we started a 30-minute emission scan 5 minutes after administration of the radiopharmaceutical and with the FDG-PET, a 7-minute emission scan was acquired at approximately 35 minutes after administration. Conversely, with the SG, a cesium-137 rotating pin source was used to obtain a 4-min transmission scan and the radiopharmaceutical (MET: 3.5 MBq/kg, FDG: 3.5 MBq/kg) was injected intravenously via the cubital vein. With the MET-PET, we started a 35-minute emission scan at the time of administration, and with the FDG-PET, a 10-minute emission scan was acquired approximately 45 minutes after radiotracer administration.

The static scans were reconstructed with attenuation correction using data from the transmission scan. The PET images were co-registered to an MRI that was performed on the same day, for better anatomical determination. Image fusion was performed by an image analysis program in combination with Dr. View/Linux image analysis software (Asahi Kasei Information System, Tokyo, Japan), using a method described by Kapouleas, et al.¹⁶⁾

In the 121 patients with various brain tumors, 10 mm circular regions of interest (ROIs)

were drawn manually with reference to the MRI which was superimposed on the PET image in normal brain structures that included the brainstem, thalamus, grey and white matter, and cerebellum, and avoided regions which were shifted or invaded by brain tumors or edema. ROIs were decided with agreement of three neurosurgeons and three radiological technologists who are experts in PET examination. As a rule, the ROIs in the grey and white matter were placed bilaterally in the frontal side of the parietal lobe in which the body of the lateral ventricles couldn't be seen (Fig.1), however if the frontal side of the parietal lobe was shifted or invaded by brain tumor or edema, the ROIs were placed toward the occipital side of the parietal lobe. The ROIs in the thalamus were placed at the center of the thalamus bilaterally in the plane in which the basal ganglia could be seen (Fig.1). Eight of the ROIs in the thalamus in NXi and eleven of those in the thalamus in SG were omitted because those were shifted or invaded by brain tumors or edema. The ROIs in the cerebellum were placed bilaterally in the plane in which the cerebellopontine angle could be seen (Fig.1), and the ROIs in the brainstem were placed in the middle pons level, as reported by Uda et al.¹⁷⁾ (Fig.1). A summary of all the ROIs are detailed in Table 2.

The ROIs in the DAs were manually drawn by tracing the tumor boundaries in an axial plane of a fusion image of the T2WI/MET-PET

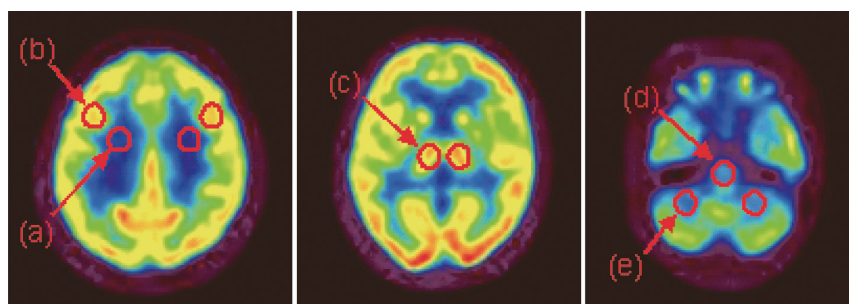


Fig.1

The ROIs placed in the normal grey matter (a), white matter (b), thalamus (c), cerebellum (d), and brain stem (e) on FDG-PET.

Table 2 Summary of all the ROIs in the normal brain structures

	The number of ROIs	
	NXi (n=66)	SG (n=55)
Evaluation of normal brain structures		
grey matter	132	110
white matter	132	110
thalamus	124	99
cerebellum	132	110
brainstem	66	55

and the T2WI/FDG-PET (Fig.2) and those in the MENs were also manually drawn by tracing the boundaries in an axial plane of a fusion image of the contrast-enhanced T1WI/MET-PET and the contrast-enhanced T1WI/FDG-PET (Fig.2).

The ROIs in the normal control cortex were manually drawn by tracing the contra-lateral frontal cortex in an axial plane of a fusion image of the T2WI/MET-PET and the T2WI/FDG-PET in which the basal ganglia could be seen (Fig.2), and in the superior and inferior axial planes of a fusion image of the T2WI/MET-PET and the T2WI/FDG-PET in which the basal ganglia could be seen. We calculated the mean SUV of the contra-lateral normal frontal cortex from three ROIs.

The regional MET and FDG uptake in the ROIs was expressed as a standard uptake value (SUV) calculated by the following formula;

$$\text{SUV} = (\text{tissue activity/ml}) / (\text{injected radio-tracer activity/body weight (g)})$$

In the MET and FDG-PET, the maximum SUV tumor/normal control cortex uptake ratios (T/N ratios) of the DAs and MENs were calculated by the following formula;

$$\text{T/N ratio} = \frac{\text{the maximum SUV of the tumor}}{\text{the average of the mean SUV of the contra-lateral normal frontal cortex}}$$

Statistical Analysis

The mean SUVs of the normal brain structures, the maximum SUVs of the DAs and the MENs, the mean SUVs of the normal control cortex, and the mean T/N ratio of the DAs and the MENs obtained from the NXi versus those from the SG were compared statistically using an independent t-test in the MET and FDG-PET, respectively. Differences with a threshold of $p < 0.05$ were considered statistically significant. All data were analyzed using SPSS 2 for Windows.

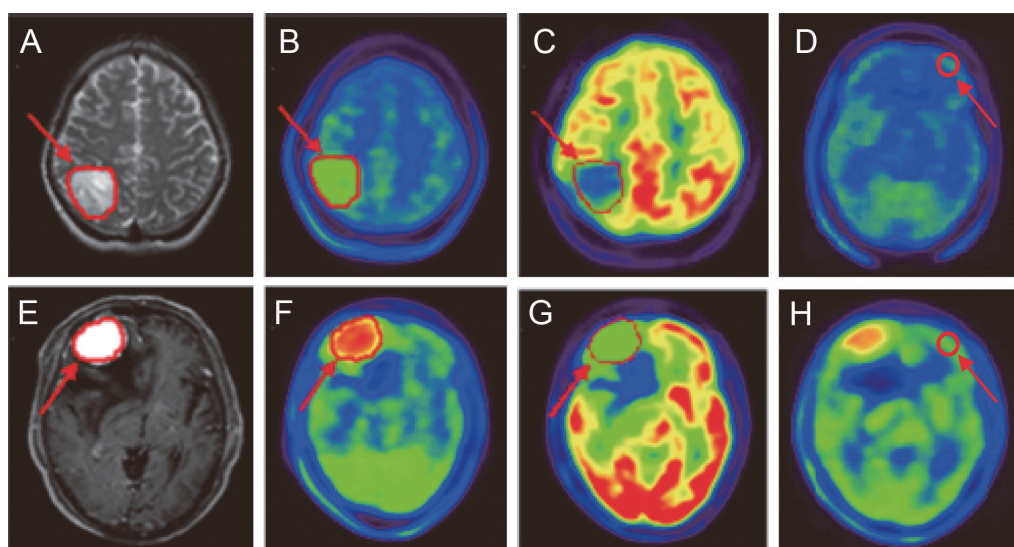


Fig.2

The ROIs placed on the T2WI (A), the MET-PET (B), and the FDG-PET (C) in a case of DA. The ROIs placed on the contrast-enhanced T1WI (E), the MET-PET (F), and the FDG-PET (G) in a case of MEN. The ROIs in the normal control cortex placed on MET-PET (D, H).

RESULTS

MET-PET

The mean (\pm SD) of the mean SUVs in the normal grey matter were 1.34 ± 0.29 versus 1.69 ± 0.45 for the NXi versus the SG, respectively. In the normal white matter the SUVs were 0.84 ± 0.20 versus 1.21 ± 0.33 , the normal thalamus, 1.47 ± 0.27 versus 2.00 ± 0.52 , the normal cerebellum, 1.59 ± 0.32 versus 1.90 ± 0.49 , and in the normal brainstem, the SUVs were 1.49 ± 0.33 versus 2.13 ± 0.56 for the 121

patients with brain tumors. The mean of the mean SUV in every normal brain structure obtained with the NXi was significantly lower than that with the SG ($p < 0.001$) (Fig.3).

In the 35 patients with DA, the mean (\pm SD) of the maximum SUV of the DAs obtained with the NXi (2.34 ± 0.74) was lower than that from the SG (2.74 ± 0.67), however this result did not reach statistical significance ($p = 0.112$) (Fig.4). The mean (\pm SD) of the mean SUV of the normal control cortex obtained with the NXi (1.13 ± 0.27) was significantly lower

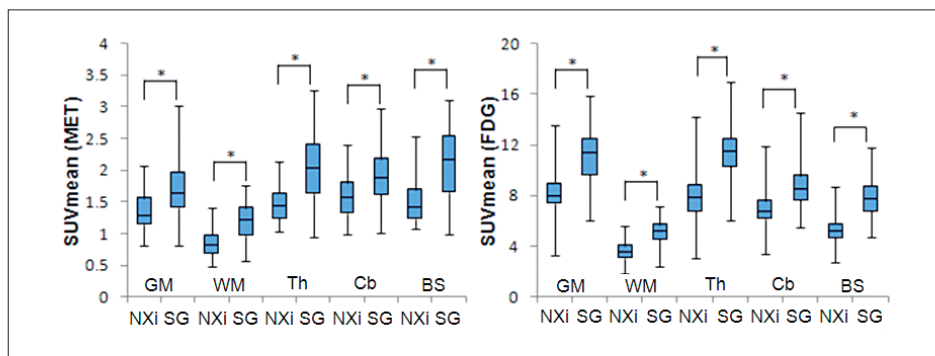


Fig.3

The mean SUVs of the normal grey matter (GM), white matter (WM), thalamus (Th), cerebellum (Cb) and brain stem (BS). Left: MET-PET. Right: FDG-PET. Box-and-whisker plots indicate the distribution (mean and SD). * $p < 0.001$.

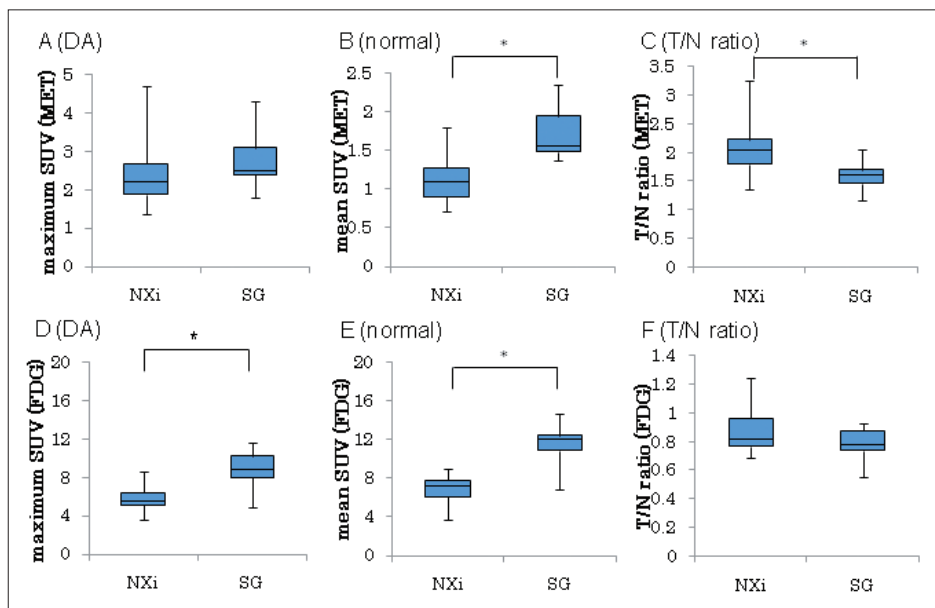


Fig.4

The maximum SUVs of the DAs (A), the mean SUVs of the normal control cortex (B) and the mean T/N ratios of DA (C) on the MET-PET. The maximum SUVs of the DAs (D), the mean SUVs of the normal control cortex (E), and the mean T/N ratios of the DAs (F) with FDG-PET. * $p < 0.001$.

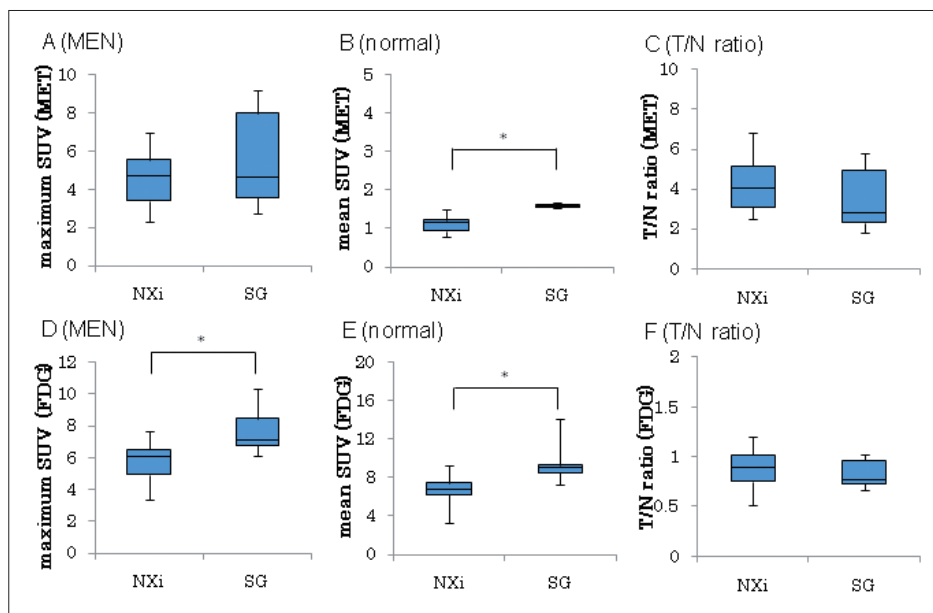


Fig.5

The maximum SUVs of the MENs (A), the mean SUVs of the normal control cortex (B) and the mean T/N ratios of the MENs (C) with MET-PET. The maximum SUVs of the MENs (D), the mean SUVs of the normal control cortex (E) and the mean T/N ratios of the MENs (F) with FDG-PET. * $p < 0.001$.

than that from the SG (1.70 ± 0.32) ($p < 0.001$) (Fig.4). The mean T/N ratio (\pm SD) of the DAs obtained with the NXi (2.09 ± 0.45) was significantly higher than the T/N ratio with the SG (1.61 ± 0.23) ($p < 0.001$) (Fig.4).

In the 19 patients with MEN, the mean (\pm SD) of the maximum SUV of the MENs obtained with the NXi (4.63 ± 1.46) was lower than the mean SUV with the SG (5.58 ± 2.80), however this result did not reach statistical significance ($p = 0.333$) (Fig.5). The mean (\pm SD) of the mean SUV in the normal control cortex obtained with the NXi (1.12 ± 0.21) was significantly lower than that with the SG (1.59 ± 0.06) ($p < 0.001$) (Fig.5). The mean T/N ratio (\pm SD) of the MENs obtained with the NXi (4.21 ± 1.36) was higher than the T/N ratio with the SG (3.50 ± 1.75), however this result also did not reach statistical significance ($p = 0.333$) (Fig.5).

FDG

The mean (\pm SD) of the mean SUVs of the normal grey matter were 8.08 ± 1.73 versus 11.17 ± 2.05 for the NXi versus the SG, respectively. In the normal white matter, the SUVs

were 3.56 ± 0.73 versus 5.08 ± 0.97 , the normal thalamus, 7.91 ± 1.85 versus 11.36 ± 2.24 , the normal cerebellum, 6.88 ± 1.39 versus 8.71 ± 1.62 , and in the normal brainstem, the SUVs were 5.19 ± 1.04 versus 7.71 ± 1.87 for the 119 patients with brain tumors. The mean SUV in every normal brain structure obtained with the NXi was significantly lower than that with the SG ($p < 0.001$) (Fig.3).

In the 35 patients with DA, the mean (\pm SD) of the maximum SUV of the DAs obtained with the NXi (5.78 ± 1.22) was significantly lower than that with the SG (8.98 ± 1.83) ($p < 0.001$) (Fig.4). The mean (\pm SD) of the mean SUV of the normal control cortex obtained with the NXi (6.79 ± 1.46) was significantly lower than that with the SG (11.25 ± 1.25) ($p < 0.001$) (Fig.4). The mean T/N ratio (\pm SD) of the DAs obtained with the NXi (0.87 ± 0.15) was increased compared to the DAs with the SG (0.78 ± 0.10), however this result also did not reach statistical significance ($p = 0.080$) (Fig.4).

In the 19 patients with MEN, the mean (\pm SD) of the maximum SUV of the MENs obtained with the NXi (5.65 ± 1.32) was signifi-

cantly lower than the SUVs with the SG (7.72 ± 1.58) ($p=0.004$) (Fig.5). The mean (\pm SD) of the mean SUV of the normal control cortex obtained with the NXi (6.66 ± 1.40) was significantly lower than that with the SG (9.51 ± 2.39) ($p=0.004$) (Fig.5). The mean T/N ratio (\pm SD) of MENs obtained with the NXi (0.87 ± 0.21) was higher than the T/N ratio with the SG (0.83 ± 0.15), however this result also did not reach statistical significance ($p=0.673$) (Fig.5).

DISCUSSION

In this study, in both the MET and FDG-PET, the mean SUV of every normal brain structure obtained with the NXi was significantly lower than those acquired with the SG. Furthermore, in patients with DA and MEN, the mean SUV of the normal control cortex with the NXi was significantly lower than that with the SG in both the MET and FDG-PET. In agreement with these results, some related studies were found in the literature. Kato, et al. reported that the mean SUV of the normal cortex with MET-PET was 1.25 ± 0.39 or 1.22 ± 0.37 , and with FDG-PET was 6.48 ± 1.51 in studies using a PET scanner with a 2D acquisition system^{14, 15}. In addition, Miyake, et al. reported that the mean SUV of the normal cortex with MET-PET was 1.52 ± 0.36 and that with FDG-PET was 8.90 ± 8.72 in their study, which used a PET scanner with a 3D acquisition system⁴. The results of these studies support our finding that the mean SUV of normal brain structures with a 2D acquisition system is lower than those obtained with a 3D acquisition system. However, the limitation of these studies is that they were performed in different patients. This finding of lower mean SUVs in normal brain structures with 2D acquisition is likely due to differences in the amount of true, scatter and random coincident radiation between 2D and 3D acquisition systems¹⁸⁻²⁰. With a 2D acquisition system, the septa, which are situated in front of the detectors of a PET scanner, can reduce not

only true scatter and random coincident radiation in the gantry, but also scattered radiation outside of the gantry.

A 3D system can detect more true coincident radiation than a 2D system, however, at the same time, a 3D system picks up more scattered and random coincident radiation that increase the image noise as compared to a 2D system. Although some devices use various image reconstruction techniques to overcome these noise issues and to improve image quality with 3D systems, the noise reduction is still sub-optimal.

In this study, the maximum SUVs in the DAs and MENs were consistently higher than the mean SUV of the contralateral normal frontal cortex in the MET-PET, however, with FDG-PET, the maximum SUVs in the DAs and MENs were consistently lower than those of the contralateral normal frontal cortex. The maximum SUVs of the DAs and MENs in FDG-PET obtained with the NXi were both significantly lower than those with the SG, although there were no significant differences between those with the NXi and SG using MET-PET. These results suggest that in cases where the SUV is the same as that of normal brain structures or less, the SUV obtained with the NXi is lower than that with the SG regardless of both tumor type and PET tracer used. However, in cases where the SUV is greater than the SUV of normal brain structures, there is no significant difference between the SUVs with the NXi versus the SG.

In the study using a 2D acquisition system by Kato, et al., the T/N ratio of DA with MET-PET was 2.24 ± 0.90 and that with FDG-PET was 0.79 ± 0.08 ¹⁴. In the study using a 3D acquisition system by Singhal, et al., the T/N ratio of DA with MET-PET was 1.56 ± 0.74 , and that with FDG-PET was 0.63 ± 0.37 ²¹. Using MET-PET of MEN, Aki, et al. reported that the T/N ratio of 5.50-6.62 was obtained using a 2D acquisition system, and in a study using a 3D acquisition system by Arita, et al., the T/N ratio

was 2.45 ± 0.67 ^{12, 22)}.

With regard to the SUV of the normal frontal cortex used as the denominator of the formula to calculate the T/N ratio, the SUV obtained with the 3D acquisition system was significantly higher than that with the 2D acquisition system in both the MET and FDG-PET. On the other hand, for the SUV of tumors as the numerator of the same formula, there was no significant difference between the SUVs from the MET-PET obtained with the 2D and 3D acquisition systems, because those are markedly higher than normal brain structures in MET-PET. However, because the SUVs of tumors in FDG-PET are lower than those of the normal brain structures, the SUV obtained with a 3D acquisition system is significantly higher than that with a 2D acquisition system as well as the SUV of normal brain structures. This finding explains why the T/N ratio obtained with a 3D acquisition system is significantly lower than that obtained with 2D acquisition system in MET-PET, however, with FDG-PET, there is no significant difference in the T/N ratio obtained with either a 2D or a 3D acquisition system.

We should note that in tumors in which the SUV is higher than that of normal brain structures in PET, the T/N ratio obtained with a 3D acquisition system is lower than that with a 2D acquisition system. However, in tumors in which the SUV is equal to or lower than that of normal brain structures, the T/N ratio obtained with a 3D acquisition system is approximately equal to that obtained with a 2D acquisition system when the measured values obtained with different PET scanners are comparatively evaluated. The results of this study may contribute to the diagnostic comparison of the results of PET examination in brain tumors not only among institutes having different PET scanners but also between data obtain from two types (2D or 3D) of PET scanners even in a single institute.

There are two limitations in this study. First, we should have enrolled identical patients for both

PET studies using the 2D and 3D acquisition systems to perform the comparative study exactly. However, because the time period when the 2D acquisition system was used in our hospital was different from the time when the 3D acquisition system was used, studies using both scanners at the same time on the same patients could not be undertaken. Second, DA and MEN were adopted as representative brain tumors in this study because these tumor types are known to have homogeneous radiotracer uptake had within the lesion. It is still uncertain whether the relationship between the tumor SUV and the difference in acquisition type (2D versus 3D) shown in this study will be true in cases of tumors with heterogeneous radiotracer uptake like glioblastoma^{23, 24)} or in tumors in which FDG has high uptake within the lesions like malignant lymphoma⁹⁾. Further investigations are warranted.

CONCLUSION

The results of this study suggest that in tumors in which the SUV was higher than that of normal brain structures in PET, the tumor SUVs obtained with a 3D acquisition system might be the same as that with a 2D resulting in a T/N ratio with 3D that might be lower than that with 2D. However, in tumors in which the SUV was the equal to or lower than that of normal brain structures, the tumor SUVs obtained with 3D might be higher than those with 2D resulting in a T/N ratio obtained with 3D that was approximately equal to that with the 2D acquisition system.

DISCLOSURE

The costs of publication of this article were defrayed in part by the payment of page charges. Therefore, and solely to indicate this fact, this article is hereby marked "advertisement" in accordance with 18 USC section 1734. This research was also supported by Gifu University

Graduate School of Medicine. No other potential conflict of interest relevant to this article was reported.

ACKNOWLEDGMENTS

We thank Dr. Tatsuki Aki, Dr. Shingo Yonezawa and Dr. Yu-ichi Nomura for their assistance with patient preparation, and also thank Mr. Ryu-ji Okumura for his assistance with the technical support.

図の説明

- Fig.1 FDG-PETの画像で正常脳の関心領域について示した。(a)が灰白質、(b)が白質、(c)が視床、(d)が小脳、(e)が脳幹を指している。
- Fig.2 びまん性星細胞腫の症例の関心領域を示しており、(A)が T_2 強調画像、(B)がMET-PET、(C)がFDG-PETに対応している。髄膜腫の症例の関心領域を示しており、(D)が T_2 強調画像、(E)がMET-PET、(F)がFDG-PETに対応している。(D)と(H)はMET-PETにおける正常脳の関心領域について図示したものである。
- Fig.3 向かって左側のグラフがMET-PET、右側がFDG-PETの平均SUVを示しており、それぞれ正常灰白質(GM)、白質(WM)、視床(Th)、小脳(Cb)、脳幹(BS)となっている。箱ひげ図で平均値と標準偏差を示している。 $*p < 0.001$
- Fig.4 びまん性星細胞腫のMET-PETの結果を示しており、最大SUVが(A)、正常脳の平均SUVが(B)、T/N比が(C)に対応している。またFDG-PETの結果は最大SUVが(D)、正常脳の平均SUVが(E)、T/N比が(F)に対応している。 $*p < 0.001$
- Fig.5 髄膜腫のMET-PETの結果を示しており、最大SUVが(A)、正常脳の平均SUVが(B)、T/N比が(C)に対応している。またFDG-PETの結果は最大SUVが(D)、正常脳の平均SUVが(E)、T/N比が(F)に対応している。 $*p < 0.001$

REFERENCES

- 1) Tietze A, et al.: Spatial distribution of malignant tissue in gliomas: correlations of ^{11}C -L-methionine positron emission tomography and perfusion - and diffusion-weighted magnetic resonance imaging. *Acta Radiol*, September 30, 2014.
- 2) Glaudemans AW, et al.: Value of ^{11}C -methionine PET in imaging brain tumours and metastases. *Eur J Nucl Med Mol Imaging*, 40: 615-635, 2013.
- 3) Galldiks N, et al.: Volumetry of [^{11}C]-methionine positron emission tomographic uptake as a prognostic marker before treatment of patients with malignant glioma. *Mol Imaging*, 11: 516-527, 2012.
- 4) Miyake K, et al.: Usefulness of FDG, MET and FLT-PET studies for the management of human gliomas. *J Biomed Biotechnol*, 2012.
- 5) Tripathi M, et al.: Comparison of F-18 FDG and C-11 methionine PET/CT for the evaluation of recurrent primary brain tumors. *Clin Nucl Med*, 37: 158-163, 2012.
- 6) Moulin-Romsée G, et al.: Non-invasive grading of brain tumours using dynamic amino acid PET imaging: does it work for ^{11}C -methionine?. *Eur J Nucl Med Mol Imaging*, 34: 2082-2087, 2007.
- 7) Pirotte B, et al.: PET imaging in the surgical management of pediatric brain tumors. *Childs Nerv Syst*, 23: 739-751, 2007.
- 8) Borbély K, et al.: Optimization of semi-quantification in metabolic PET studies with ^{18}F -fluorodeoxyglucose and ^{11}C -methionine in the determination of malignancy of gliomas. *J Neurol Sci*, 246: 85-94, 2006.
- 9) Yamaguchi S, et al.: the diagnostic role of (18)F-FDG PET for primary central nervous system lymphoma. *Ann Nucl Med*, 28: 603-609, 2014.
- 10) Okochi Y, et al.: Clinical use of ^{11}C -methionine and ^{18}F -FDG-PET for germinoma in central nervous system. *Ann Nucl Med*, 28: 94-102, 2014.
- 11) Cremerius U, et al.: Fasting improves discrimination of grade 1 and atypical or malignant meningioma in FDG-PET. *J Nucl Med*, 38: 26-30, 1997.
- 12) Aki T, et al.: Evaluation of brain tumors using dynamic ^{11}C -methionine-PET. *J Neurooncol*, 109: 115-122, 2012.
- 13) Takenaka S, et al.: Comparison of ^{11}C -methionine, ^{11}C -choline, and ^{18}F -fluorodeoxyglucose-PET for distinguishing glioma recurrence from radiation necrosis. *Neural Med Chir (Tokyo)*, 54: 280-289, 2014.
- 14) Kato T, et al.: Metabolic Assessment of Gliomas Using ^{11}C -methionine, [^{18}F] Fluorodeoxyglucose, and ^{11}C -choline Positron-Emission Tomography. *Am J Neuro-radiol*, 29: 1176-1182, 2008.
- 15) Kato T, et al.: Analysis of ^{11}C -methionine uptake in low-grade gliomas and correlation with proliferative activity. *Am J Neuroradiol*, 29: 1867-1871, 2008.
- 16) Kapouleas, et al.: Registration of three-dimensional MR and PET images of the human brain without markers. *Radiology*, 181: 731-739, 1991.
- 17) Uda, et al.: Evaluation of the accumulation of (11)C-methionine with standardized uptake value in the normal brain. *J Nucl Med*, 51: 219-222, 2010.
- 18) MacDonald LR, et al.: Effective count rates for PET scanners with reduced and extended axial field of view. *Phys Med Biol*, 56: 3629-3643, 2011.
- 19) Macdonald LR, et al.: Measured count-rate performance of the Discovery STE PET/CT scanner in 2D, 3D and partial collimation acquisition modes. *Phys Med Biol*, 53: 3723-3738, 2008.
- 20) Lartzien C, et al.: Optimization of injected dose based on noise equivalent count rates for 2- and 3-dimensional whole-body PET. *J Nucl Med*, 43: 1268-1278, 2002.
- 21) Singhal T, et al.: ^{11}C -methionine PET for grading and prognostication in gliomas: a comparison study with ^{18}F -FDG PET and contrast enhancement on MRI. *J Nucl Med*, 53: 1709-1715, 2012.
- 22) Arita H, et al.: Clinical characteristics of meningiomas assessed by ^{11}C -methionine and ^{18}F -Fluorodeoxyglucose positron-emission tomography. *J Neurooncol*, 107: 379-386, 2012.
- 23) Aubry M, et al.: From the core to beyond the margin: a genomic picture of glioblastoma intratumor heterogeneity. *Oncotarget*, 2015.
- 24) Sottoriva A, et al.: Intratumor heterogeneity in human glioblastoma reflects cancer evolutionary dynamics. *Proc Natl Acad Sci U S A*, 110: 4009-4014, 2013.